Observation of a critical gradient threshold for electron temperature fluctuations in the DIII-D tokamak

J.C. Hillesheim[1], J.C. DeBoo[2], W.A. Peebles[1], T.A. Carter[1], G. Wang[1], T.L. Rhodes[1], L. Schmitz[1], G.R. McKee[3], Z. Yan[3], G.M. Staebler[2], K.H. Burrell[2], E.J. Doyle[1], C. Holland[4], C.C. Petty[2], S.P. Smith[2], A.E. White[5], and L. Zeng[1]

[1]*Department of Physics and Astronomy, University of California, Los Angeles, CA, USA*
[2]*General Atomics, San Diego, CA, USA*
[3]*University of Wisconsin, Madison, Madison, WI, USA*
[4]*University of California, San Diego, La Jolla, CA, USA*
[5]*Massachusetts Institute of Technology, Cambridge, MA, USA*

A significant issue for magnetic confinement fusion devices is the cross-field transport of particles, momentum, and heat by gyroradius-scale turbulence. This turbulence is widely thought to arise due to linear instabilities. Many of these gyroradius-scale modes are expected to exhibit a threshold in the equilibrium gradient providing free energy for the instability, where the mode is linearly stable below the threshold and unstable above [1].

We present direct, systematic evidence of a critical gradient threshold in a locally measured turbulence characteristic in the core of a tokamak; namely, we observe a threshold in the inverse electron temperature scale length, $L_{T_e}^{-1} = -\nabla T_e/T_e$, above which electron temperature fluctuations, $\delta T_e/T_e$, abruptly increase. In contrast, measurements of the density fluctuation level show no definite threshold. Additional turbulence measurements and comparison to linear gyrofluid predictions can be found in Ref. [2]. Previous similar studies investigated only indirect evidence [3]. Unlike previous work investigating ion heat transport [4], these observations are not very sensitive to toroidal rotation. A critical threshold was concurrently observed for electron thermal transport, which had a weak dependence on rotation.

The experiment was performed in the DIII-D tokamak [5] and was designed to investigate electron profile stiffness and critical gradients [6]. Plasmas were in L-mode, MHD-quiescent, upper single null diverted, with plasma current $I_p = 0.8$ MA, minor radius $a \approx 0.6$ m, major radius $R_0 \approx 1.7$ m, $B_0 = 2$ T toroidal magnetic field (directed opposite to I_p), and had line-averaged density of $\sim 2 \times 10^{13}$ cm^{-3}. The resonance locations of six gyrotrons used for electron cyclotron heating (ECH) were switched shot-to-shot between $\rho = 0.5$ and $\rho = 0.7$, which scanned $L_{T_e}^{-1}$ at $\rho = 0.6$. In addition to ECH-only cases, neutral beam injection (NBI) was employed to create the $L_{T_e}^{-1}$ scans at three rotation states: two co-injected (to I_p) NBI sources (ECH+Co-NBI), two counter-injected NBI sources (ECH+Ctr-NBI), and balanced injection with one of each (ECH+Bal-NBI). Combinations of NBI and ECH were held in steady-state for 500-800 ms. One ECH source at $\rho = 0.7$ was modulated at 50% duty cycle for transient heat pulse analysis; this had a neglible effect on the turbulence measurements at $\rho = 0.6$. There was ~ 3 MW ECH power in all shots. NBI periods had ~ 2 MW of beam power.

Figure 1 shows the response of the equilibrium T_e and $L_{T_e}^{-1}$ profiles to ECH location for the ECH-only case, where unambiguous critical gradient behavior was observed. By keeping the

total ECH power constant while gyrotrons were re-steered shot-to-shot, T_e changed little for $\rho > 0.7$. The change in $L_{T_e}^{-1}$ was predominantly due to ∇T_e; T_e also increased, but was restricted to the range of 0.7 to 0.9 keV at $\rho = 0.6$.

The local toroidal rotation at $\rho = 0.6$ (near midplane on the low field side) was varied from 10 ± 6 km/s for ECH+Ctr-NBI to 58 ± 4 km/s for ECH+Co-NBI (given values are average plus or minus the standard deviation for all ECH arrangements), with the two other cases in between. Flow shear also varied but was small in all cases. There are $\sim 25\%$ uncertainties in plotted values of $L_{T_e}^{-1}$. Further transport analysis, turbulence data, and equilibrium information are being published separately [2, 6].

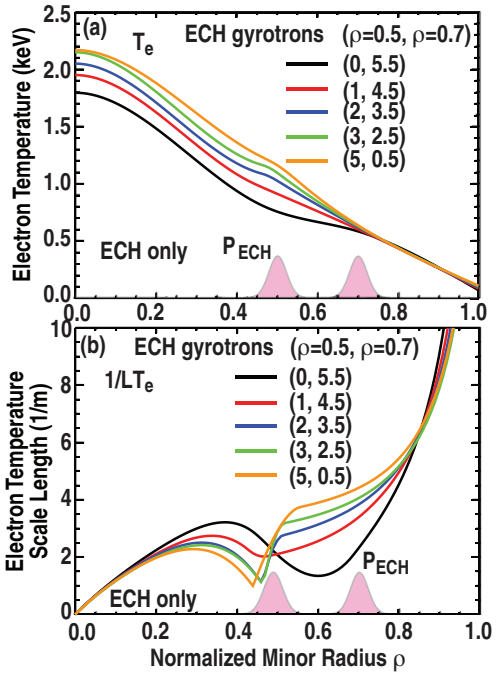

Figure 1: Response of (a) electron temperature profile and (b) inverse scale length profile to ECH location for ECH-only case. ECH power deposition profiles are annotated.

Measurements of $\delta T_e/T_e$ were acquired with a correlation electron cyclotron emission (CECE) radiometer [7]. The CECE system's four channels were arranged to acquire $\delta T_e/T_e$ at two radial locations, $\rho \approx 0.55$ and $\rho \approx 0.61$; the plasma was optically thick ($\tau > 10$) for the ECE measurements. Beam emission spectroscopy (BES) [8] measured density fluctuations, $\delta n/n$, during the ECH+CO-NBI case. All reported turbulence measurements are long wavelength ($k_\theta \rho_s \lesssim 0.5$, ρ_s is the ion sound gyroradius and k_θ is the poloidal wavenumber).

The principal result is shown in Fig. 2, where both the local electron heat flux, Q_e, and $\delta T_e/T_e$ increase rapidly above a critical value of $L_{T_e}^{-1}$. The electron heat flux inferred from power balance analysis [9] for the data set is plotted in Fig. 2(a), normalized to the gyro-Bohm flux, $Q_{GB} = n_e T_e c_s (\rho_s/a)^2$, where $c_s = \sqrt{T_e/m_i}$. The heat flux increases nonlinearly with $L_{T_e}^{-1}$, similar to Ref. [3]. Figure 2(b) shows $\delta T_e/T_e$ measurements: a threshold value is observed, below which $\delta T_e/T_e$ is unchanged (within uncertainties, given by the detection limit of the diagnostic [10, 11]), and above which it abruptly increases by a factor of ~ 2. This observation is consistent with the trapped electron mode (TEM) instability [12] that is characterized by growth rates proportional to $L_{T_e}^{-1}$. It should be noted that while $\delta T_e/T_e$ increases by a factor of ~ 2, Q_e increases by more than a factor of 10; this is discussed further in Ref. [2]. In comparison to $L_{T_e}^{-1}$, rotation and flow shear have little effect on either the inferred heat flux or $\delta T_e/T_e$ measurements. The normalized collision frequency, $\nu^* = \nu_{ei}/(c_s/a)$ (ν_{ei} is the electron-ion collision frequency), is ~ 0.1 at the measurement locations and β (ratio of plasma pressure to magnetic field pressure) is $< 0.5\%$, which places the experiment in a TEM relevant regime.

Measurements of $\delta n/n$ from BES, depicted in Fig. 2(b), at $\rho \approx 0.58$ in the ECH+Co-NBI scan show a $\sim 20\%$ increase from the minimum $L_{T_e}^{-1}$ to the next lowest value, above which $\delta n/n$ shows little change. The increase in the ratio $(\delta T_e/T_e)/(\delta n/n)$ is consistent with a transition to predominantly TEM turbulence [13].

Taking the electron thermal diffusivity, χ_e, to be proportional to $(\delta T_e/T_e)^2$ and using a functional form similar to Ref. [14], the $(\delta T_e/T_e)^2$ data was fit to

$$c_0 + c_1 \left(L_{T_e}^{-1} - L_{T_e}^{-1}|_{crit}\right)^{\ell} H\left(L_{T_e}^{-1} - L_{T_e}^{-1}|_{crit}\right), \quad (1)$$

where $H(x)$ is the Heaviside function. By varying $(\delta T_e/T_e)^2$ within uncertainties, the average and standard deviation of an ensemble of fits resulted in $L_{T_e}^{-1}|_{crit} = 2.8 \pm 0.4$ m^{-1}. The average fit is shown in Fig. 2(b).

A critical gradient for χ_e was found for ECH-only plasmas using transient heat pulse analysis [6] at $L_{T_e}^{-1}|_{crit} = 3.0 \pm 0.2$ m^{-1}, which is within uncertainties of the value for $\delta T_e/T_e$.

Analytical predictions for the critical threshold for ∇T_e-TEM have been investigated. It has been argued in previous work that zonal flows have little influence on ∇T_e-TEM turbulence [15, 16], consequently little non-linear upshift of the critical gradient is expected and the experiment can be compared to linear predictions. The Weiland fluid model was used to find [17]

$$\left.\frac{R}{L_{T_e}}\right|_{crit} = \frac{20}{9K_t} + \frac{2}{3}\frac{R}{L_n} + \frac{K_t}{2}\left(1 - \frac{R}{2L_n}\right)^2, \quad (2)$$

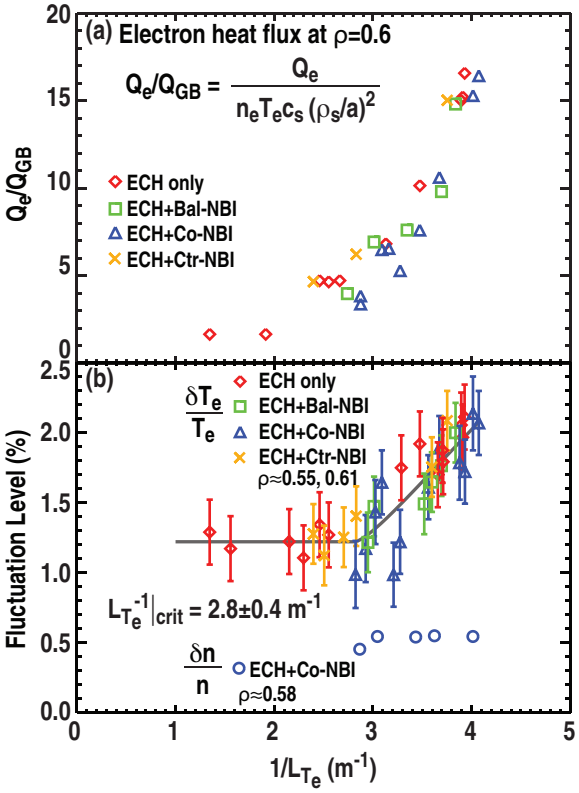

Figure 2: (a) Electron heat flux at $\rho = 0.6$ from transport analysis and (b) electron temperature and density fluctuations as a function of $|\nabla T_e|/T_e$, with fit plotted.

where $K_t = f_t/(1 - f_t)$ and f_t is the fraction of trapped electrons. Evaluating Eq. (2) over the entire data set at $\rho = 0.6$ results in a mean and standard deviation of $L_{T_e}^{-1}|_{crit} = 1.7 \pm 0.2$ m^{-1}, which is significantly lower than the value of $L_{T_e}^{-1}|_{crit} = 2.8 \pm 0.4$ m^{-1} found for $\delta T_e/T_e$. Since the model Eqn. 2 is derived from lacks full description of kinetic electrons, collisions, shaping, and other effects, disagreement is perhaps not surprising. Effects not captured in Eq. (2), *e.g.* T_e/T_i dependence, are also discussed in Ref. [17].

Another formula for the ∇T_e-TEM is given in Ref. [18]; there, parameter scans of linear gyrokinetic simulations with quasilinear flux calculations were performed at a value of $L_{T_e}^{-1}$ around twice the critical value, with extrapolation assuming a linear dependence between flux

and gradient to determine $L_{T_e}^{-1}|_{crit}$. The result was

$$\left.\frac{R}{L_{T_e}}\right|_{crit} = \frac{0.357\sqrt{\varepsilon}+0.271}{\sqrt{\varepsilon}}\left[4.90-1.31\frac{R}{L_n}+2.68\hat{s}+ln\left(1+20\nu_{eff}\right)\right] \quad , \qquad (3)$$

where ε is the inverse aspect ratio, $\hat{s}$ is the magnetic shear, and $\nu_{eff} = 0.1 n_e^* Z_{eff}/T_{keV}^2$, where n_e^* is the electron density in units of 10^{19} m^{-3} and T_{keV} is the electron temperature in units of keV. Evaluating Eq. (3) for the data set at $\rho = 0.6$ yields $L_{T_e}^{-1}|_{crit} = 4.6 \pm 0.2$ m^{-1}, also in quantitative disagreement with the experiment. Given that the electron heat flux in Fig. 2(a) clearly increases faster than linearly, it is qualitatively consistent that one would expect Eq. (3) to over-predict the critical gradient value. Equation (3) also includes no shaping effects. It is notable that in other work it has been argued that Eq. (3) did describe the experimentally observed gradient over $0.4 \lesssim \rho \lesssim 0.8$ in QH-mode DIII-D plasmas [19]. It is not clear why disagreement is found for the L-mode plasmas here — future investigations are warranted.

We have reported the direct observation of a critical gradient threshold for a locally measured turbulence characteristic in the core of a tokamak in a systematic experiment. Both analysis of electron thermal transport and measurements of electron temperature fluctuations show a critical threshold in $L_{T_e}^{-1}$ and little sensitivity to rotation or rotation shear: the clear inference is that the $\delta T_e/T_e$ increase plays a causal role for the increased transport and profile stiffness. Quantitative disagreement is found with analytical estimates of the ∇T_e-TEM threshold. Comparisons to gyrofluid and gyrokinetic predictions are presently being pursued.

This work was supported by the US Department of Energy under DE-FG03-01ER54615, DE-FG02-08ER54984, DE-FC02-04ER54698, DE-FG02-95ER54309, DE-FG02-89ER53296, DE-FG02-08ER54999, DE-FG02-06ER54871, DE-FG02-07ER54917, and DE-FC02-93ER54186.

References

[1] W. Horton, Rev. Mod. Phys. **71**, 735 (1999)
[2] J.C. Hillesheim *et al.*, "Observation of a critical gradient threshold for electron temperature fluctuations in the DIII-D tokamak," submitted to Phys. Rev. Lett. (2012).
[3] F. Ryter *et al.*, Phys. Rev. Lett. **95**, 085001 (2005)
[4] P. Mantica *et al.*, Phys. Rev. Lett. **102**, 1750002 (2009)
[5] J.L. Luxon, Nucl. Fusion **42**, 614 (2002)
[6] J.C. DeBoo *et al.*, "Electron profile stiffness and critical gradient studies," submitted to Phys. Plasmas (2012)
[7] A.E. White *et al.*, Rev. Sci. Instrum. **79**, 103505 (2008)
[8] G.R. McKee *et al.*, Rev. Sci. Instrum. **70**, 913 (1999)
[9] H.E. St. John *et al.*, Plasma Phys. Control. Nucl. Fusion Research **3**, 603 (1994)
[10] G. Cima *et al.*, Phys. Plasmas **2**, 720 (1995)
[11] A.E. White *et al.*, Phys. Plasmas **17**, 056103 (2010)
[12] B.B. Kadomtsev *et al.*, Nucl. Fusion **11**, 67 (1971)
[13] A.E. White *et al.*, Phys. Plasmas **17**, 020701 (2010)
[14] F. Imbeaux *et al.*, Plasma Phys. Control. Fusion **44**, 1425 (2002)
[15] T. Dannert and F. Jenko, Phys. Plasmas **12**, 072309 (2005)
[16] D.R. Ernst *et al.*, Phys. Plasmas **16**, 055906 (2009)
[17] A. Casati *et al.*, Phys. Plasmas **15**, 042310 (2008)
[18] A.G. Peeters *et al.*, Phys. Plasmas **12**, 022505 (2005)
[19] L. Schmitz *et al.*, Nucl. Fusion **52**, 023003 (2012)